RF-FOCUSED SPOKE RESONATOR*

R. W. Garnett, F. L. Krawczyk, R. L. Wood, and D. L. Schrage
Los Alamos National Laboratory, Los Alamos, NM 87545, USA

Abstract

In this paper we discuss the feasibility of using finger-like structures added to a superconducting spoke resonator cavity to superimpose a modest amount of electric quadrupole focusing onto the high axial accelerating field. The motivation for this idea is to eliminate the need for magnetic focusing elements such as solenoids between spoke cavities in a cryomodule at very low beam velocities and thereby improving the real-estate accelerating gradient by increasing the longitudinal packing factor. So far, proposed linac designs using spoke resonators at low-β have not been able to fully take advantage of the high gradients available due to the high longitudinal phase advance per period caused by engineering constraints. Preliminary results of cavity modeling and analytical calculations for the proposed structure will be discussed.

1 INTRODUCTION

A first attempt at a "proof-of-principle" design of a spoke resonator with quadrupole focusing is discussed. Simulation results using Microwave Studio (MSW) to determine the electromagnetic properties of this cavity are presented. The results of both analytical and TRACE 3-D calculations used to estimate the net focusing achievable for this geometry are also presented.

2 RF-FOCUSING SPOKE RESONATOR

The geometry of our RF-focusing spoke resonator is based on a preliminary design of a β=0.125 multi-gap 350-MHz resonator simulated for the Advanced Accelerator Applications Project [1]. We assume a 3-gap 2-spoke cavity; the center gap of a 3-gap 2-spoke cavity automatically provides the required electrical and mechanical symmetry needed for a quadrupole in the shortest cavity length. We have modified the center gap to produce a quadrupole-focusing field in addition to the axial accelerating field of the cavity. Table 1 gives some geometric details of the modified spoke structure. The overall cavity dimensions are not given since this cavity is not yet optimized for overall RF performance.

Initially, a simple electrostatic model was used to examine, to first order, the behavior of various proposed gap and aperture shapes. The shape that produced the cleanest axial-plus-quadrupole field was judged to be too difficult to build out of Niobium. Additionally, this geometry has pockets where cryogen vapor could collect and where chemical etching mixtures could pool. The

---

geometry shown in Fig. 1 was selected as a good compromise since it appears to produce an adequate quadrupole contribution, does not have the drainage problems, and appears to be less complex to build.

Table 1 - Cavity geometry data (left end of cavity at 0.0).

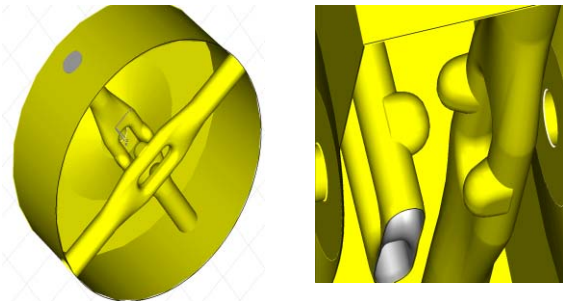| Physical length	13.39286 cm	w/o flanges
Center of 1st gap	2.232 cm	short, no quad
Center of 2nd gap	06.843 cm	long, with quad
Center of 3rd gap	11.161 cm	short, no quad
Aperture Radius	1.0 cm	

Figure 1 - Spoke geometry cut-away views.

An expanded view of the center gap of the spoke resonator is shown in Fig. 1. It is modified in the following ways to produce a quadrupole-focusing field component: First, the beam apertures in the spokes are elongated transversely from the original 20 mm circular opening to a slot 20 mm across, and up to 100mm long. The edges of the slot are rounded as were those of the circular opening. This elongation, by itself, contributes an almost insignificant amount of quadrupole field [2]. The "finger" protrusions into the accelerating gaps produce most of the quadrupole effect. Without the slots, the peak surface fields, and the cavity capacitance are much too high.

2.1 Microwave Studio (MWS) Analysis Results

Table 2 gives the transit-time factor as a function of proton beam velocity for the proposed spoke cavity. Acceptable acceleration efficiency is achieved with this cavity in spite of the introduction of a quadrupole focusing field component. Table 3 gives the expected RF performance of this non-optimized resonator as determined by the MWS simulations. None of these data are unreasonable. Nevertheless, the peak surface electric field needs to be improved to achieve reasonable gradients without problems. The quadrupole-focusing strength of this particular design appears to be high. Reducing the quadrupole focusing strength somewhat and optimizing the structure geometry will lower the peak

surface fields of the structure. Figure 2 shows the electric field for the accelerating/focusing mode from MWS.

Table 2 - Transit-time factor vs. proton beam velocity.

β	Transit-Time Factor
0.090	0.5913
0.110	0.7786
0.120	0.7990
0.140	0.7675
0.160	0.6953
0.180	0.6155
0.200	0.5404

Table 3 - Cavity RF data.

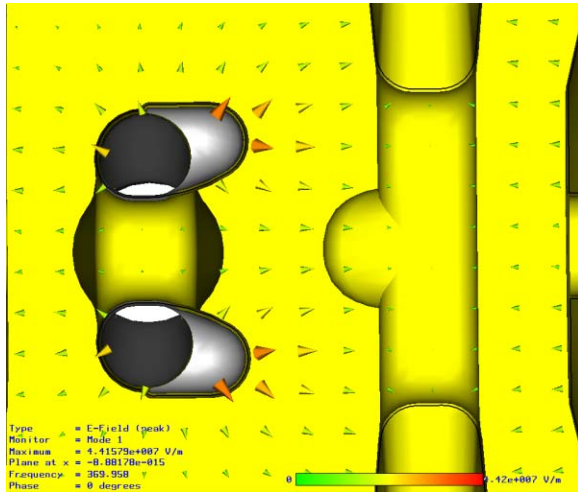| Q_0 (RT)	8907
ZT^2/Q	311 Ω
G	44.69 Ω
Q_0 (4K)	7.33E+008
E_p/E_a	14.27
B_p/E_a	170 G/MV/m

Figure 2 - The electric field for the accelerating/ focusing mode.

To estimate the quadrupole strength of the RF-field solution, we examined the volume electric field data from MWS and matched them to a 3-D analytical model for superimposed axial and transverse quadrupole fields. However, this was not acceptable since the field distribution contains more spatial harmonics than the electrostatic model predicted. Instead, we used the MWS data to estimate the integrated effects of the axial and transverse fields on particles passing through the gap at a fixed x-y location. On the central axis, the voltage ($\int E_Z dz$) for this one gap is roughly 537 kV for the excitation level chosen. This increases gradually with increasing x (for y=0) to 564 kV at x=9mm (nominal aperture radius = 10mm). The $\int E_x dz$ from one side of the gap to the other was also calculated for various trajectories: (x, y) = (0-9mm,0), in 1-mm steps in x. Out to x=7mm, this integral increased very linearly at a rate of

26.2 kV/mm. At larger radii, the rate of increase of the integral begins to roll-off. In a pure quadrupole field, this value would continue to increase linearly. The roll-off is indicative of weak higher-order spatial modes. We did not attempt to quantify these higher-order spatial modes at this time, since the gap shape has not yet been optimized, and since we did not have a good way to assess their effects on the beam. We will, of course, set maximum limits on the magnitude of these harmonics as part of the optimization process, just as is done in quadrupole magnet designs. Figure 3 shows a plot of the variation of $\int E_x dz$ with radius.
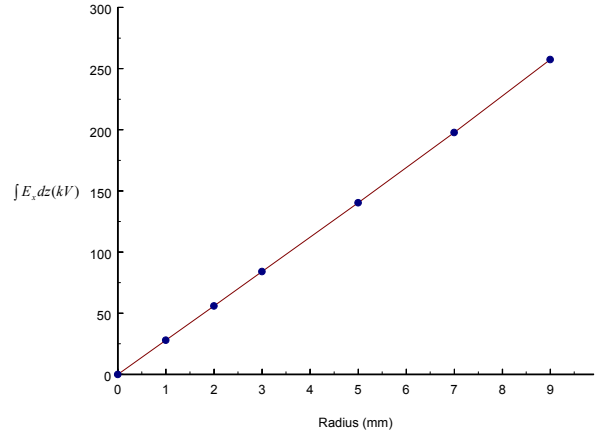

Figure 3 - $\int E_x dz$ as a function of radius.

2.2 Estimate of Quadrupole Focusing Strength

We have used the following expression to estimate the transverse zero-current phase advance per period σ_{0t} in the smooth approximation for singlet electric quadrupole focusing in the spoke cavity [3]:

$$\left(\frac{\sigma_{0t}}{2L}\right)^2 = \left(\frac{e\int E_x dz}{2m\gamma\beta^2 c^2 a}\right)^2 - \frac{\pi e(E_0 T)\sin(-\phi)}{mc^2\lambda\gamma^3\beta^3}.$$

The second term in the above equation is the RF-defocusing term. The focusing period length is 2L, E_x is the pole-tip electric field, a is the aperture radius, $E_0 T$ is the axial accelerating gradient, and ϕ is the synchronous phase.

Figure 4 shows σ_{0t} as a function of period length for various accelerating gradients. As can be seen, with the present cavity focusing geometry it is easy to exceed 90° of transverse zero-current phase advance per period. At high gradients it will be necessary to reduce the transverse focusing strength by adjusting the position of the finger-like structures in each resonator to the desired value for a specified focusing period length. As an example, for an accelerating gradient of 5 MV/m the present focusing strength must be reduced by approximately a factor of 8 in order to reduce σ_{0t} to approximately 80° for a period length of 0.868 m. This assumes that the physical length of the cavity is 0.134 m, as described in the previous section, and that 0.3 m is required to fit the helium vessel

and tuner mechanism between the cavities [4]. Of course, as the beam energy increases the net electric focusing decreases.

Figure 5 shows σ_{ot} as a function of β for EoT=5 MV/m, a synchronous phase angle of -30°, and the focusing period given above. Additionally, the poor transit-time factor for these cavities at high energies, make them impractical for use over this large energy range. Figure 5 merely indicates that strong electric focusing is possible over a rather large energy range using the proposed focusing scheme. The relative strength of the quadrupole focusing to the RF defocusing was also found to be high for reasonable accelerating gradients and synchronous phase angles.
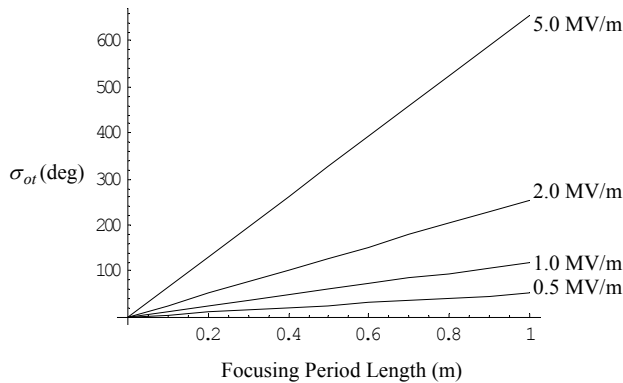

Figure 4 – Zero-current transverse phase advance per period as a function of period length for various accelerating gradient values.
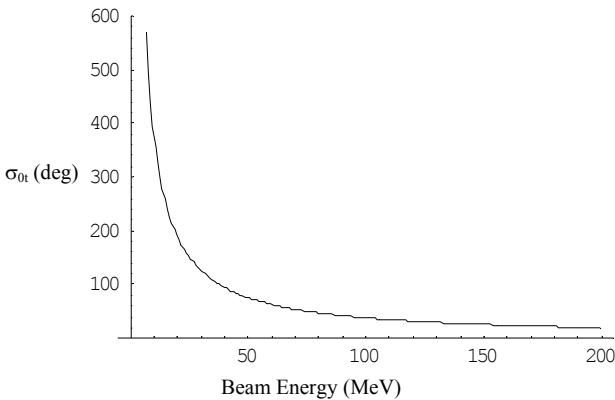

Figure 5 – Zero-current transverse phase advance per period as a function of beam energy for EoT=5 MV/m, a focusing period of 0.868 m, and a synchronous phase of -30°.

At present, most of our simulation codes, including TRACE 3-D, do not model electric focusing elements. However, an expression for the equivalent magnetic quadrupole can be found by setting the expressions for the zero-current transverse phase advance per period for the two cases equal and solving for the equivalent magnetic quadrupole gradient G, as a function of the pole-tip electric field:

$$G = \frac{E_x}{\beta ca} \approx \frac{\int E_x \, dz}{\Delta z} \frac{1}{\beta ca},$$

where Δz is the gap length of our cavity which is equal to 0.05357m. As an example, using TRACE 3-D simulations for a beam energy of 6.7 MeV and assuming our 0.868-m focusing period, an equivalent magnetic quadrupole gradient of 22.0 T/m is required to achieve σ_{ot} of approximately 80°. Using this equivalent gradient value in the above equation gives, $\int E_x \, dz = 3.78 \times 10^5$ volts for the required field integral. Therefore, for a given beam energy and cavity bore radius, it is the value of the field integral that must be maintained in order to achieve the desired focusing for all values of EoT by modifying the focusing geometry in the cavity.

TRACE 3-D was also used to estimate the ratio of beam aperture radius to rms size as a function of current for our example focusing lattice in order to understand the useful current range for this approach. Ratios of 6.6, 5.0, and 3.8 were obtained for the following beam current (transverse emittance) combinations: 13.3 mA (0.0152), 49.27 mA (0.0183), and 94.32 (0.0263), respectively. The transverse emittances are normalized and have units of π-cm-mrad. These RFQ output emittances were calculated previously for the APT/AAA Project using PARMTEQM. Assuming the present cavity bore radius of 1.0 cm, use of this focusing approach may be practical for beam currents near 10 mA. However, more detailed beam dynamics calculations will be required.

The idea we are presenting in this paper is not entirely original. References 2 and 5 describe similar structure approaches. Encouraging experimental results from 1990 for a split-ring resonator with the addition of RFQ vanes ("fingers") are presented in Ref. 6 and indicate that we have a high probability of achieving the accelerating and focusing fields determined from our simulations. However, eventually our results must be verified by prototyping and testing the structure we are proposing.

3 REFERENCES

[1] F. Krawczyk et al., "Design of a Low-β, 2-Gap Spoke Resonator for the AAA Project," Proceedings of the 2001 Particle Accelerator Conference, Chicago, Illinois, June 18-22, 2001

[2] P. Lapostolle, Compt. Rend. Vol. 256 (1963), p. 5294-5297.

[3] T. Wangler, "RF Linear Accelerators," John Wiley & Sons, Inc., 1998, p. 220, equation 7.103.

[4] P. Kelley et al., "ADTF Spoke Cavity Cryomodule Concept," Los Alamos National Laboratory Report LA-UR-01-3818, July, 2001.

[5] V.V.Vladimirskii, Probory i Tekhn. Eksperim, Vol.3 (1956), p. 35.

[6] J. R. Delayen and K. W. Shepard, "First Tests of a Superconducting RFQ Structure," Proceedings of the 1990 Linear Accelerator Conference, Albuquerque, New Mexico, September 10-14, 1990, p.76.